CHAPTER FOUR

Drug-Target Binding Forces: Advances in Force Field Approaches

PETER A. KOLLMAN
University of California
School of Pharmacy
Department of Pharmaceutical Chemistry
San Francisco, California

DAVID A. CASE
The Scripps Research Institute
Department of Molecular Biology
La Jolla, California

Contents

1 Introduction, **170**
2 Energy Components for Intermolecular Noncovalent Interactions, **171**
  2.1 Electrostatic Energy, **171**
  2.2 Exchange Repulsion Energy, **172**
  2.3 Polarization Energy, **173**
  2.4 Charge Transfer Energy, **173**
  2.5 Dispersion Attraction, **174**
  2.6 Summary, **174**
3 Molecular Mechanics Force Fields, **174**
  3.1 Biochemical Force Fields, **175**
  3.2 Force Field Models for Simple Liquids, **176**
  3.3 Nonadditive and More Complex Models, **176**
  3.4 Long Range Electrostatic Effects, **177**
4 Thermodynamics of Association, **177**
  4.1 Gas Phase Association, **177**
  4.2 Solvation Effects, **177**
  4.3 An Illustrative Example: Protonation of Amines, **179**
5 Calculating Free Energies, **180**
6 Examples of Drug-Receptor Interactions, **181**
  6.1 Biotin-Avidin, **181**
  6.2 Dihydrofolate Reductase–Trimethoprim, **183**
  6.3 Nucleotide Intercalator, **183**
7 Summary, **183**

Burger's Medicinal *Chemistry* and Drug Discovery
Sixth Edition, Volume **1:** Drug Discovery
Edited by Donald J. Abraham
ISBN 0-471-27090-3 © **2003** John Wiley & Sons, Inc.

1 INTRODUCTION

This chapter describes the forces that hold together complexes between large and small molecules, particularly where the large molecule is a protein or nucleic acid and the small molecule is an inhibitor or substrate. Forces between atoms are conventionally divided into the two categories of covalent and noncovalent "bonds." A covalent bond is an attractive interaction between two atoms in which each contributes a valence electron. For example, such a bond is formed between two hydrogen atoms to make the H, molecule: H + H → H-H. It also includes what most chemists might consider "ionic" bonds such as Na + Cl → Na-Cl, even though the valence electron pair in this case is much closer to the chlorine atom than to the sodium atom. The conventional study of chemical reactions is devoted to describing the strengths of covalent bonds and to understanding the ways in which they are formed and broken (1).

Drug–receptor interactions, on the other hand, are generally influenced most by weaker, noncovalent "bonds," where electron pairs are "conserved" in reactants and products. Examples of such interactions are "dative bonds," e.g., $H_3N: + BH_3 \rightarrow H_3N{:}BH_3$ and hydrogen bonds, e.g., $H_2O + H_2O \rightarrow H_2O\cdots HOH$. It is these noncovalent bonds that provide the "force" to make drugs interact strongly with their targets.

Some sample potential energy curves for covalent and noncovalent interactions between two atoms are given in Fig. 4.1. The left side shows an interaction curve for the two oxygen atoms in the O_2 molecule. This has a large dissociation energy D_o (about 117 kcal/mol in this case), so that at room temperature where RT approximates 0.6 kcal/mol (R is the universal gas constant and T is the absolute temperature), the fraction of "broken" bonds at equilibrium $e^{-D_o/RT}$ is very small. By contrast, noncovalent bonds are much weaker, typically 1-10 kcal/mol, and thus much easier to break. The right side of Fig. 4.1 shows interaction curves for the two sodium atoms in the Na_2 dimer; this interaction is somewhat stronger than a typical hydrogen bond but has about the same shape. Also shown is the purely nonbonded interaction between two oxygen atoms in different water molecules. Here the D_o value is so small (about 0.15 kcal/mol) that it really cannot be seen on the scale of this figure. Hence, a significant fraction of nonbonded interactions can be broken at equilibrium at room temperature. It is this weakness of noncovalent bonds that makes them so useful in biological processes, because a small change in the chemical environment (such as temperature, concentrations, or ionic strength) can form or break such a bond. Probably the best known important noncovalent bonds are those between the strands of DNA, where hydrogen bonds hold the double helix together. When the cells begin to replicate, chemical signals (e.g., proteins binding to the DNA) shift the equilibrium to the single-stranded DNA, breaking these hydrogen bonds. Other important examples of noncovalent complexes include those between enzyme and substrate, "receptor" protein and hormone, antibody and antigen, and intercalator and DNA.

Much of our concern in this chapter is with the interaction:

$$\text{drug} + \text{receptor} \underset{k_r}{\overset{k_f}{\rightleftarrows}} \text{complex}$$

The rate constant for association of the complex is k_f; the rate constant for dissociation of the complex is k_r; and the affinity, or association constant $K_{as} = k_f/k_r$. It is usually assumed that the biological activity of a drug is related to its affinity K_{as} for the receptor, although there are processes such as actinomycin D-DNA interactions in which the rate of dissociation k_r is more relevant to the biological activity (2, 3).

The thermodynamic parameters of interest for the reactions above are the standard free energy ($\Delta G°$), enthalpy ($\Delta H°$), and entropy

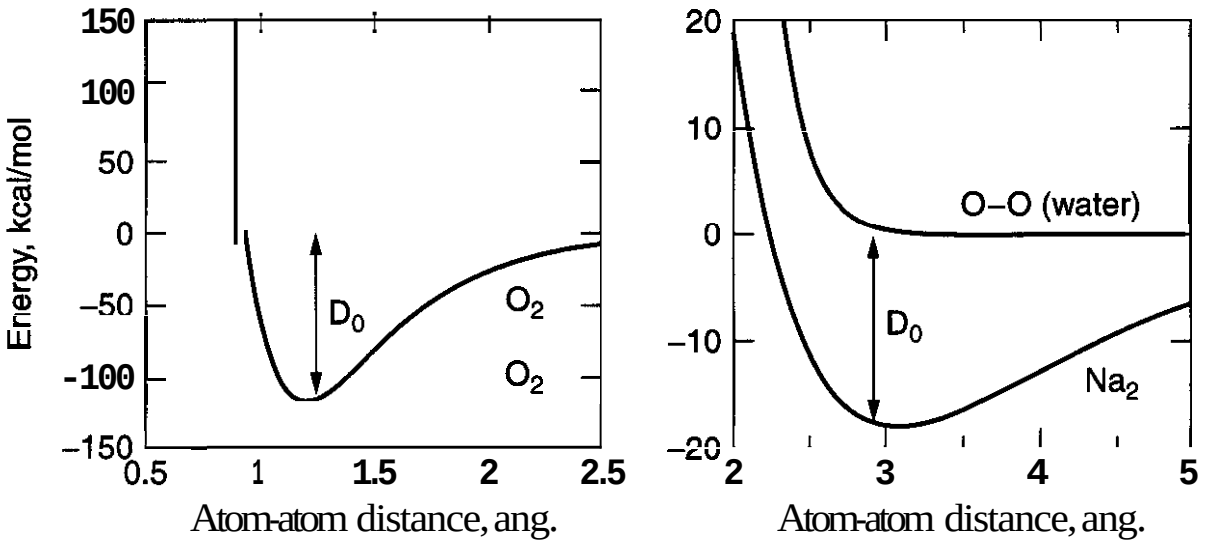


Figure 4.1. Potential energy curves for atom–atom interactions in O_2, Na_2, and the O—O interaction in a water dimer. Note the different energy scales on the left and right.

(AS") of association. These are related by the equations

$$\Delta G^\circ = -RT \ln K_{as}$$

$$\Delta G^\circ = AH^o - T\Delta S^\circ$$

This measurement of K_{as} allows one to calculate ΔG°, the free energy of association of the complex. To find ΔH° and ΔS° separately requires a determination of K_{as} as a function of temperature (if AH" and AS" are relatively temperature independent, a plot of ln K_{as} vs. $1/T$ can yield ΔH° and ΔS°) or a calorimetric measurement of AH" directly. Because AH^o and AS" themselves are often quite temperature dependent, the latter experiment is more definitive.

This chapter provides some background about the forces that hold molecules together, with emphasis on the noncovalent interactions of interest in biology, and attempts to relate experimental determinations of the thermodynamics of association to the forces involved in the association. The discussion in the remainder of the chapter is divided into two parts. First, we discuss the forces that hold molecules together in the gas phase and solution and describe how these forces can be mathematically modeled by fairly simple functions; second, we discuss biological examples of noncovalent interactions and analyze the binding forces in particular cases.

2 ENERGY COMPONENTS FOR INTERMOLECULAR NONCOVALENT INTERACTIONS

Quantum mechanical calculations on small molecule association suggest that there are five major contributions to the energy of intermolecular interactions in the gas phase (3, 4). The sum of these is the dissociation energy of the intramolecular complex represented in Fig. 4.1. Table 4.1 contains some examples of magnitudes of the different energy components for different interactions. This section provides a qualitative introduction to these forces. Section gives and overview of mathematical models suitable for computer calculations.

2.1 Electrostatic Energy

Given information on the charge distribution of two molecules A and B, we can evaluate the electrostatic interaction energy between them. Although nuclei can be treated as point positive charges, the negative charge of electrons is smeared out over space. Thus, a rigorous evaluation of the electrostatic energy involves an integration over the electron clouds of the two molecules. In most practical calculations, however, the electrons as well as the nuclei are represented by point charges, whose position and magnitude are usually chosen to reproduce known molecular properties. The strength and the directionality of A. . .B electrostatic interactions are usually

Table 4.1 Some Examples of Interaction Energies of Noncovalent Complexes (kcal/mol)

Interaction	Interaction Energies					
	$-\Delta E \equiv D_o$	ΔE_{es}	ΔE_{dis}	ΔE_{ex}	ΔE_{pol}	ΔE_{ct}
He . . . He	0.02[a]	0	−0.028	+0.008	0	0
Xe . . . Xe	0.64[a]	0	−0.86	0.40	0	0
$C_6H_6 \ldots C_6H_6$	≈2[b]	≠0	≠0	≠0	≠0	≠0
$H_2O \ldots H_2O$	8.9[c]	−9.2	(−1)	4.0	−0.5	−2.2
TCNE . . . OH,	4.1[d]	−3.9	(−1)	2.0	−0.2	−1.0
$Li^+ \ldots OH_2$	48.9[e]	−51.1	(−1)	12.7	−7.8	−1.7
$F^- \ldots OH$,	41.1[e]	−37.8	(−1)	20.5	−4.9	−17.9
$NH_4^+ \ldots F^-$	164.7	−181.4	(−1)	61.6	−8.3	−35.6

$-\Delta E$, calculated (or experimental) total interaction energy equal to D_o in Fig. 1, kcal/mol; AE_{es}, electrostatic energy; ΔE_{dis}, dispersion energy; AE_{ex}, exchange repulsion energy; ΔE_{pol}, polarization energy; AE_{ct}, charge transfer energy (values in parentheses are estimated; TCNE, tetracyanoethylene).

[a] See Karplus and Porter (12).

[b] See Janda et al. (13).

[c] See Umeyama and Morokuma (7); this value for AE is certainly too large; see better values in Table 3.

[d] See Morokuma et al. (13).

[e] See Kollman (14).

dominated by the first nonvanishing multipole moment $\mathbf{M}_n$ of the charge distribution,

$$\mathbf{M}_n = \sum_{i=1}^{\text{no. charges}} q_i \mathbf{r}_i^n$$

where q_i are the individual charges and $\mathbf{r}_i$ is the vector from the origin of the coordinate system to the ith charge (5, 6). Molecules that are charged have a nonzero zeroth moment M_o. Ionic crystals such as Na^+Cl^- are held together predominantly by electrostatic attraction between oppositely charged ions. Crystals of ice I are mainly held together by dipolar electrostatic forces where $\mathbf{M}_0 = 0$ and $\mathbf{M}_1 \neq 0$, because there are virtually no ions in these crystals. It should be noted here that "hydrogen bonding" is not a separate energy component; typically hydrogen bonds contain important energy contributions from all five energy components, although the electrostatic component is usually the largest contributor to this interaction (7).

Of the intermolecular energy components, the electrostatic is the longest range (i.e., it dies off most slowly with distance as the two molecules separate). Ion–ion interactions die off as $1/R$; ion–dipole as $1/R^2$; dipole–dipole as $1/R^3$, etc. In general, if two molecules have as their first nonvanishing multipole moments $\mathbf{M}_n$ and $\mathbf{M}_m$, the electrostatic interaction energy between them dies off as $1/R^{n+m+1}$. The electrostatic interaction energy between water a dipolar molecule ($n = 1$) and benzene, whose first nonvanishing moment is a quadrupole ($m = 2$), dies off as $1/R^4$.

2.2 Exchange Repulsion Energy

The Pauli principle keeps electrons with the same spin spatially apart. This principle applies whether one is dealing with electrons on the same molecule or on different molecules and is the predominant repulsive force (6) that keeps electrons of different molecules from interpenetrating when noncovalent complexes are formed. This repulsive term is often represented by an analytical function of the form

$$\frac{A}{R^n} \quad n = 9 \text{ or } 12$$

where R is the distance between molecules or nonbonded atoms and A is a constant that depends on the atom types. However, the best available quantum mechanical calculations suggest that this repulsion should diminish with an exponential dependence on the distance between the atoms (6). This difference is only important for very precise calculations: the key point is that the repulsive energy rises very quickly once the electrons from two different atoms overlap significantly. Roughly speaking, this happens with the distance be-

Table 4.2 Selected Atomic van der Waals Radii (in Å)

Element	r_{VDW}
Hydrogen	1.20
Carbon	1.70
Nitrogen	1.55
Oxygen	1.50
Fluorine	1.50
Phosphorus	1.85
Sulfur	1.80
Chlorine	1.70
Bromine	1.80

Values from A. Bondi, *J. Phys. Chem.* 68,441 (1964).

tween two atoms is less than the sum of their van der Waals radii. Table 4.2 gives some typical radii for atoms commonly found in organic molecules.

2.3 Polarization Energy

When two molecules approach each other, there is charge redistribution within each molecule, leading to an additional attraction between the molecules. The energy associated with this charge redistribution is invariably attractive and is called the polarization energy. For example, if a molecule with polarizability a is placed in an electric field, E, the polarization energy is

$$E_{pol} = -\frac{1}{2}\alpha \mathbf{E}^2$$

If the electric field is caused by an ion, then $E = qi/R^2$, where q is the ionic change, i is the unit vector along the ion–molecule direction, and R the ion–molecule distance, which is the $E_{pol} = -1/2\alpha q^2/R^4$ for this ion-induced dipole interaction. The corresponding formula for *dipole*-induced dipole interaction between two dipolar molecules is

$$E_{pol} = -\frac{1}{2}\frac{\alpha_1\mu_2^2 + \alpha_2\mu_1^2}{R^6}$$

where the μ's are the dipole moments of the molecules, the a's are their polarizabilities, and R is the distance between molecules. The polarizability of a molecule can be broken down into atomic contributions [atomic polarizabilities are additive to a good approximation (8)], and it is roughly proportional to the number of valence electrons, as well as on how tightly these valence electrons are bound to the nuclei. Umeyama and Morokuma (9) have calculated the ion-induced dipole contribution to the proton affinities of the simple alkyl amines. They attributed the order of gasphase proton affinities in the alkyl amines [$NH_3 < CH_3NH_2 < (CH_3)_2NH < (CH_3)_3N$] to the greater polarizability of a methyl group than a hydrogen. A simple estimate using the above empirical equation for an ion-induced dipole interaction with q = +1, which is the difference in polarizabilities of a methyl and a hydrogen ($\Delta\alpha$) $\approx$ 4 cm^3, a proton–methyl distance of 2.0 Å, and a proton–proton distance of 1.6 Å, leads to an expected increase of ~20 kcal/mol of proton affinity for every methyl group added to NH_3. This very qualitative estimate is of the right magnitude but about two to three times too large (see below).

2.4 Charge Transfer Energy

When two molecules interact, there is often a small amount of electron flow from one to the other. For example, in the equilibrium geometry of the linear water dimer HO—H. . .OH_2, the water molecule that is the proton acceptor has transferred about $0.05e^-$ to the proton donor water (9, 10). The attractive energy associated with this charge transfer is the charge transfer energy and can be thought of as a mixing of an ionic resonance structure $H—O^{(-)}. . .H——OH_2^{(+)}$ into the overall wave function. Although the charge transfer energy is an important contributor to the interaction energy of most noncovalent complexes, the presence of a "charge transfer" electronic transition in the visible spectrum does not mean that the charge transfer energy is the predominant force holding the complex together in its ground state. For example, the complex between benzene and I_2, earlier thought to be a prototype "charge transfer" complex, seems to be held together predominantly by electrostatic, polarization, and dispersion energies in its ground electronic state (11).

2.5 Dispersion Attraction

There are attractive forces existing between all pairs of atoms, even between rare gas atoms (He, Ar, Ne, Kr, Xe), which cause them to condense at a sufficiently low temperature. None of the other attractive forces (electrostatic, polarization, charge transfer) can explain the attraction between rare gas atoms; it is called the dispersion attraction (12). Even though the rare gas atoms have no permanent dipole moments, they are polarizable, and one has instantaneous dipole–dipole attractions in which the presence of a locally asymmetric charge distribution on one molecule induces an asymmetric charge distribution on the other molecule, e.g., $'-He^{S}+ \ldots '-He^{S}+$.

The net attraction is called dispersion attraction (often known as London or van der Waals attraction) and is dependent on the polarizability and the number of valence electrons of the interacting molecules. It dies off as $1/R^6$, where R is the atom–atom separation. The difference between this attraction and the polarization energy is that the latter involves the interaction of a molecule that is already polar with another polar or nonpolar molecule.

2.6 Summary

Having described the components of the interaction energies, let us consider a number of specific examples in detail (Table 4.1). Unlike the total interaction energy, which can be measured experimentally, the individual energy components cannot. The theoretical estimate of these quantities is often dependent on the method of calculation, but their qualitative features are usually independent of methodology.

Rare gas–rare gas interactions (He. . .He and Xe. . .Xe) have only ***dispersion*** attraction. The difference between the potential well depth of He. . .He and Xe. . .Xe (Fig. 4.1; D_o) at the equilibrium distance is caused by the greater polarizability of the xenon atoms, and thus to the greater dispersion attraction between them. A simple manifestation of this is the much higher boiling point of xenon than helium, caused by the greater attractive forces in xenon liquid. Although these energies are individually fairly small, they can add in a molecular environment to significant energies; for example, the single largest attractive free energy contribution to binding in the strongest known small molecule–macromolecule interaction (biotin-avidin) is the dispersion attraction **(13).**

One might intuitively expect that benzene dimer would pack together like two flat plates, but this is not the case in the gas phase (14); the crystal structure also does not have parallel alignments of benzene molecules (15). Benzene, although having no dipole moment, does have a ***quadrupole*** moment ($\mathbf{M}_2 \neq 0$). A simple way to think about this quadrupole moment is to realize that a benzene C—H is somewhat electropositive and its electron cloud is rather electronegative. A second benzene molecule would like to approach the first one so that its "electropositive" side approaches the other molecule's "electronegative side." Hence the main component of binding is expected to be electrostatic in nature. The water dimer $(H_2O)_2$ and the ether. . .TCNE interactions are examples of prototypal H bonds and "charge transfer" complexes, but both are also held together mainly by electrostatic forces, although the other attractive energy components contribute significantly to the total ΔE. The electrostatic component is predominant in determining all the structural parameters except the distance between molecules. Similarly, the geometry and net attraction between Li^+ and OH,, F^- and H_2O, and NH_4^+ and F– are dominated by the electrostatic energy component.

3 MOLECULAR MECHANICS FORCE FIELDS

We move now from qualitative considerations to a more quantitative approach. It has become clear that a simple molecular mechanical energy expression can represent noncovalent interactions surprisingly well (16). Such energy expressions contain only the first three terms mentioned above: electrostatic, exchange repulsion, and dispersion. By a suitable choice of parameters, change transfer and polarization effects are implicitly included in such an expression, which is simple and easy to evaluate, along with its derivatives, for

molecules with thousands of atoms. Over the past quarter century, many interesting applications of such molecular mechanical methods to complex molecules have been carried out (17).

The ideas that are outlined in a qualitative way above can also be cast into a useful mathematical form for computer calculation. The basic idea is to write down a (fairly simple and approximate) function that gives the energy of the system as a function of the positions (or coordinates) of its atoms. Because the derivative (or gradient) of this function yields the forces for Newton's equations, such a function is often called a "force field"; and because molecules are viewed as being made up of balls and springs (so that quantum effects are ignored), the term "molecular mechanics" is used to represent a concrete, mechanical picture of molecular motions and energies.

3.1 Biochemical Force Fields

Equation 4.1 represents about the simplest functional form of a force field that preserves the essential nature of molecules in condensed phases.

$$
\begin{aligned}
U(\mathbf{R}) &= \sum_{\text{bonds}} K_r(r - r_{\text{eq}})^2 && \text{bond} \\
&+ \sum_{\text{angles}} K_\theta(\theta - \theta_{\text{eq}})^2 && \text{angle} \\
&+ \sum_{\text{dihedrals}} \frac{V_n}{2}\,(1 + \cos[n\phi - \gamma]) && \text{dihedral} \\
&+ \sum_{i<j}^{\text{atoms}} \frac{A_{ij}}{R_{ij}^{12}} - \frac{B_{ij}}{R_{ij}^{6}} && \text{van der Waals} \\
&+ \sum_{i<j}^{\text{atoms}} \frac{q_i q_j}{\varepsilon R_{ij}} && \text{electrostatic}
\end{aligned}
\qquad (4.1)
$$

The earliest force fields, which attempted describe the structure and strain of small organic molecules, focused considerable attention on more elaborate functions of the first two terms, as well as cross terms (18), representing a "top down" philosophy.

On the other hand, biochemists, guided by an interest in proteins and nucleic acids, have more generally followed a "bottom up" approach (16, 19, 20). This approach focuses first on the atomic charges q_i. The most general method to derive the atomic charges is to fit them to quantum mechanically calculated electrostatic potentials on appropriately chosen molecules or fragments. In early attempt to do this, computational limitations in quantum mechanical calculations led to the use of a minimal basis set STO-3G to derive the q_i (16). More recent efforts have used a 6-31G* or larger basis set (19). The 6-31G* basis set has the fortunate property in that it leads to charges (dipole moments) that are enhanced over accurate gas phase experimental values, and thus, implicitly builds in "polarization" effects characteristic of polar molecules in condensed phases. The fact that this basis set enhances the polarity just about the same amount as the popular water models TIP3P (21) and SPC (22), (where the charges are empirically adjusted to reproduce the water enthalpy of vaporization) is a fortunate fact and is key in leading to balanced solvent–solvent and solvent–solute interactions.

van der Waals parameters are generally dominated by the inner closed shell of electrons and thus are fortunately far more transferable than atomic charges. Therefore, gener-

ally only one set of van der Waals parameters (radius and well depth) per atom type need be employed, with the important exception of hydrogen (23). Unfortunately, it is harder to derive van der Waals parameters than charges using ab *initio* quantum mechanics (6, 24). The alternative that has emerged as a general model is to empirically calibrate results to fit experimental liquid structures and enthalpies (25).

Continuing with the "bottom up" development of a force field, we come to the torsion energy term, where the V_n and γ either come from experiment or quantum mechanical calculations on small molecule models. Whereas "top down" force fields often use many terms in the Fourier series for rotation around a given bond type and attempt to reproduce the conformational energy for a collection of molecules, most "biochemical" force fields take a minimalist approach (16, 19, 20). For example, we would have only a single V_3 torsional term around an X-C-C-Y bond except when X or Y are electronegative, where another term can be rationalized from electronic effects and can be derived directly using quantum mechanical calculations. This helps our model to be more easily generalized to new molecules, albeit in some cases probably at the cost of some accuracy. Exceptions to this minimalist approach are the ψ, ϕ of peptides and χ of nucleic acids, where more terms were added to ensure as accurate as possible a reproduction of the conformational energies around these key bonds.

Finally, to ensure reasonable representation of bond and angle terms, we use empirical data (structures and vibrational frequencies). The use of this simple harmonic model precludes high accuracy, but in our opinion, one would compromise the simplicity and generality of the model with more complex functional forms.

3.2 Force Field Models for Simple Liquids

A key test of this approach is the ability to accurately reproduce liquid structures and energies and free energies of solvation; these have traditionally been considered as key elements in the development of successful force fields for liquids (25). The aqueous solvation free energies of a large number of molecules, including substituted benzenes, methanol, hydrocarbons, N-methyl acetamide, and dimethyl sulfide, as well as the liquid structure and energy of methanol and N-methyl acetamide, show good agreement with experiment, with little or no adjustment of parameters. For example, Fox and Kollman (25) have shown that this approach leads to a density and enthalpy of vaporization of liquid dimethyl sulfoxide (DMSO) within 2% of experiment, using restrained electrostatic potential charges (RESP) and van der Waals parameters taken without modification from the corresponding values in proteins. Similar results have been obtained for other organic liquids.

3.3 Nonadditive and More Complex Models

What are the most important weaknesses in the above-described parameterizational approach and the use of Equation (4.1)? In our opinion, the main ones are the use of an effective two-body potential and the use of only atom-centered charges.

$$E_{\text{pol}} = -\frac{1}{2}\sum_{i}^{\text{atom}} \mu_i \cdot \mathbf{E}_i^{(o)} \quad \text{polarization} \quad (4.2)$$

where μ_i is atomic polarizability. Substantial progress has been made in laying the foundation for the development of a complete force field including explicit nonadditive effects (adding Equation 4.2 to Equation 4.1). First, we have shown that such models, in contrast to additive models, lead to good agreement with experimental solvation free energies of representative organic ions $CH_3NH_3^+$ and $CH_3CO_2^-$ without any adjustment of van der Waals parameters (26). Second, we have shown that such nonadditive terms are essential in accurately describing cation–π interactions (27). Third, we have shown that one can equally well describe liquid CH_3OH and *N*-methyl-acetemide (NMA) with additive models or a nonadditive model in which the charges are uniformly reduced (by 0.88) (28). Finally, the interaction free energy of Li+ with hexaanisole spherand is more accurately described by nonadditive than additive molecular mechanical models (29). In addition, considering off-center charges in electrostatic potential fit models of atoms with "lone pairs"

shows that they can often be important in leading to very accurate description of H bond directionality (30).

3.4 Long Range Electrostatic Effects

To accurately describe the energy and structure of complex systems, not only are the functional form and parameters of molecular models described by Equations 4.1 and 4.2 important, but also the manner in which the long range electrostatic effects are represented. The standard approach is to use a nonbonded cutoff for both electrostatic and van der Waals interactions, which seems to be a reasonable method for proteins but seems to be a poor method to describe highly charged molecules such as nucleic acids. For periodic systems, Ewald methods (which are too complex to be described here) have been known for a long time to remove most of the artefacts arising from cutoffs, and impressive efficiency and accuracy of a variant called particle-mesh Ewald (PME) has been demonstrated for protein crystals (31) [0.3 Å rms deviation from the observed crystal structure for bovine pancreatic trypsin inhibitor (BPTI) in a 1-ns simulation with an increase in computer time of only ~50% over standard cutoff methods]; the PME method also leads to accurate simulations of proteins, DNA, and RNA in solution (32).

4 THERMODYNAMICS OF ASSOCIATION

We have focused mainly on the energy of association between molecules; in any drug- receptor interaction, we typically want to know the equilibrium constant for association K_{as} and the free energy of association AGO. The difference between the free energy (AGO) and energy ($\Delta E°$) of association is given by $\Delta G° = AH'' - TAP$, and $AH'' = \Delta E° + (\Delta PV)$. For gas phase associations, (ΔPV) is $\sim -RT$, which is −0.6 kcal/mol at room temperature. Thus, this term, when added to AE, favors association (the more negative AG, the greater tendency for association). However, AS, the entropy of association, is typically large and negative. The reason is that one is reducing the "floppy" degrees of freedom, which have large translational and rotational entropies, by six (six translations and six rotations in the free molecules, three of each in the complex) during complex formation, and replacing these with vibrations, which have lower entropies (33).

4.1 Gas Phase Association

For example, at 300 K, two CH_4 molecules have a translational entropy of 69 eu (entropy unit, or cal/K) and a rotational entropy of 31 eu, whereas $(CH_4)_2$ has a translational entropy of 37 eu and a rotational entropy (assuming a C. . .C distance of 4 & of 22 eu. Thus, one can see that the translational and rotational entropy contributions to the reaction $2CH_4 \rightarrow (CH,)$, is −41 eu. These six degrees of freedom become vibrations in the complex $(CH_4)_2$, and as such, might contribute a vibrational entropy of about 20–30 eu. Thus, for the dimerization of CH_4 in the gas phase, we expect TAS" of about −3 to −6 kcal/mol at 300 K.

As stressed in the second law of thermodynamics, the tendency for a chemical process to occur is governed both by the energy released (exothermicity) in the process and the entropy gained (the tendency of the reaction to go to a more random, disordered state). In the case of gas phase association, the energy term is invariably exothermic if the reactants approach each other in an appropriate orientation, and the entropy term is always negative, opposing association. Table 4.3 gives an example of the thermodynamics of association of water molecules in the gas phase. As one can see, the entropy (AS") contribution to association of water molecules in the gas phase is substantial and negative; thus, there is little tendency for water molecules to associate in the gas phase at room temperature and 1 atm pressure, even though the hydrogen bond energy is about 5 kcal/mol.

4.2 Solvation Effects

The thermodynamic cycle (Fig. 4.2) illustrates the problems we face in transferring our knowledge of gas phase intermolecular interactions to solution phase phenomena.

Our real interest is in AG„ the solution phase free energy of association. Until now, our discussion has focused on the energy (ΔE_1), enthalpy (AH,), and free energy (ΔG_1)

Table 4.3 Thermodynamic Functions for Gas Phase Association of Water Molecules: $2H_2O \rightarrow (H_2O)_2$

Thermodynamic Function	Value for H_2O Dimerization (kcal/mol)
$\Delta E°$ (0 K)[a]	−6.2
AE" (300 K)[a]	−4.2
AH° (300 K)[a]	−5.2
AS" (300 K)[b]	−9.0
$\Delta G°$ (300 K)	+3.8

"See Joesten and Schaad (13).

[b]Estimated using the vibration frequencies employed by Joesten and Schaad (14).

of association in the gas phase. To be able to calculate ΔG_4, we need to know ΔG_3, the solvation free energy of the drug-receptor complex; ΔG_{2D}, the solvation free energy of the drug; and AG, the solvation free energy of the receptor. These solvation free energies are the free energies gained (or lost) by taking the molecule from a standard concentration in the gas phase to a corresponding concentration in solution. Using the thermodynamic cycle in Fig. 4.2, it follows that

$$\Delta G_4 = \Delta G_1 - \Delta G_{2D} - \Delta G_{2R} + \Delta G_3 \quad (4.3)$$

Similar relationships hold for AH, and AS,. There is no reason to expect ΔG_4 and AG, to be similar, so we face the problem of estimating ΔG_{2D}, AG, and ΔG_3. We cannot measure ΔG_{2R} or ΔG_3, because this would require us to vaporize a measurable amount of a receptor or drug-receptor complex. For most polar and ionic drugs, AG, is not measurable either. Therefore, one resorts to measuring the free energy of transfer from octanol to water ΔG_{2D}(oct) rather than the free energy of transfer from the gas phase to water, ΔG_{2D}. This situation underlies the postulate of the Hansch approach (34), which suggests that the differences in ΔG_{2D}(oct) [$\Delta\Delta G_{2D}$(oct)] may be related to the biological activity of drugs, and in many cases this desolvation (water → octanol) does indeed seem to be related to drug binding and/or biological activity.

Because the individual free energies in Equation 4.3 are so hard to measure, one is led to smaller model systems to analyze the major driving force for drug- receptor association, a step taken by Kauzmann (35) in his classic paper on the forces that affect protein stability and structure. He examined the thermodynamics of association and solution of small nonpolar molecules in aqueous solution. The associations were characterized by a large *positive* entropy term and the solution by a large negative entropy, with the enthalpy terms less important. Thus, the well-known lack of solubility of hydrocarbons in water was not caused by a net loss of hydrogen bonds; the hydrocarbons cause the water molecules to become more ordered (thus to lose entropy) so that they can still find a good hydrogen bond partner (AH of solution of these hydrocarbons is often negative, but much smaller in magnitude than the TAS of solution). By coming together in aqueous solution, these hydrocarbons "release" some H_2O's, and this favorable TAS association is the driving force for this association. It is generally agreed that this "hydrophobic" effect of hydrocarbon groups is a key feature in many drug-receptor associations. A lucid description of hydrophobic forces is given by Jencks (36) and Dill (37).

Computer simulation approaches have proven very useful in enabling calculation of the association of molecules. For example, the association of two methane molecules in the gas phase would lead to a $\Delta E°$ (0 K) of ~−1 kcal/mol, and by analog with water dimer (Table 4.3), a very positive $\Delta G°$ (300 K) and thus no tendency for association. In aqueous solution, one can calculate, using modern statistical mechanical simulation methods, the potential of mean force for association of two molecules, which is the free energy as a function of molecular separation in solution. Although there is some controversy about

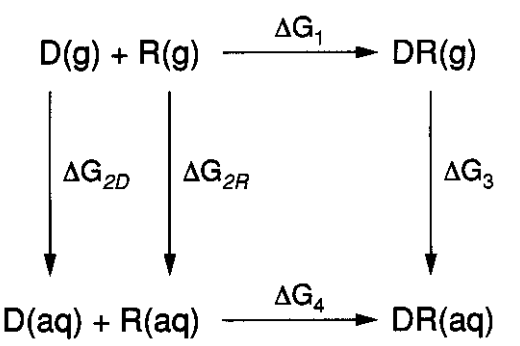


Figure 4.2. A schematic representation of the thermodynamic cycle for molecular association in the gas phase and in solution.

whether there are both "solvent-separated" and "contact" minima for two methane molecules in aqueous solution, there is no question that methane association is quite attractive in aqueous solution compared with the gas phase (38).

One can also apply such approaches to study association of ionic and polar molecules. For example, the association of Na^+ and Cl^- has a free energy of association that is very small in magnitude, in contrast to the gas phase (39). The association of two amides through a C=O . . . H–N hydrogen bond is very favorable in *vacuo* and progressively less favorable in non-polar and aqueous solution (40). Thus, water has a significant "leveling" effect on association, making nonpolar associations more favorable and ionic and polar associations less favorable than their gas phase counterparts.

Let us now summarize the foregoing discussion. Unlike the gas phase association, where AH, and AS, are invariably negative, for the corresponding thermodynamics in solution, AH, and AS, can be of either sign. The enthalpy of association AH, of two molecules in solution will bepositive if the interactions of the solvent with the uncomplexed drug and receptor are sufficiently stronger and more exothermic (AH, – AH, – ΔH_{2R} is more positive than AH, is negative) than are the interactions of the solvent with the drug-receptor complex. Similarly, the entropy of association in solution AS, can be positive if AS, – AS, – ΔS_{2R} is more positive than AS, is negative. This can come about if the entropy gain from release of solvent from its interaction with the isolated drug and receptor is sufficiently larger than the entropy gain from release of solvent from the drug receptor complex.

An additional important point to keep in mind is that the solution phase thermodynamics may be dominated (as in the case of the hydrophobic effect, the association of nonpolar solutes in water) by changes in *solvent–*solvent interactions in the presence of solute.

It is also important to stress that even an analysis of the relative contributions of AH and AS to AG may not give definitive insight into the "nature" of the drug-receptor bond. For example, a large positive AS (and small negative AH) for association might come from either a hydrophobic or an ionic association (35). In either case, the driving force for association is likely "release" of H_2O from "tight" binding to the solute.

One final consideration in determining either gas phase or solution phase association constants of drug-receptor complexes is conformational flexibility. Medicinal chemists have often attempted to synthesize rigid drug of different stereochemistries in the hopes of finding one that fits "perfectly" into the receptor site. If, for example, the drug has three equal energy conformations and only one can fit the receptor site, a price must be paid of $\Delta G = +RT \ln 3$ in binding free energy relative to the drug that is "locked" in the right conformation. If the receptor has to be locked in a conformation to "accept" the drug, one must pay a similar free energy price. A nice example of the latter situation is the difference in binding free energies between "locked" and "unlocked" macrocyclic crown ethers (41) that bind $t\text{-}BuNH_3^+$ cation.

4.3 An Illustrative Example: Protonation of Amines

Before we turn to some examples of drug-receptor interactions, let us present a specific example of the difference between gas phase and solution interactions. We choose the protonation of amines, because of the large literature that attempted to explain the irregular order of p*Ka*'s of the alkyl amines [NH_3 = 9.25; CH_3NH_2 = 10.66; $(CH_3)_2NH$ = 10.73; and $(CH_3)_3N$ = 9.811. This reaction can be represented as

$$\Delta G_1$$

$$R_3N + H^+ \rightarrow R_3N^+H$$

in the gas phase and

$$\Delta G_4$$

$$R_3N(aq) + H^+(aq) \rightarrow R_3NH^+(aq)$$

in aqueous solution. As we noted in connection with Fig. 4.2, the difference between the free energies of protonation in solution and the gas phase is given by

Table 4.4 Free Energies in Cycle (Fig. 4.2) for Protonation of Alkyl Amines (kcal/mol)[a]

R_3N	ΔG_1	$\Delta G_2(H^+)$	$\Delta G_2(R_3N)$	$\Delta G_3(R_3NH^+)$	ΔG_4
NH_3	−198.0	269.8	−2.41	−78.0	−3.79
CH_3NH_2	−210.0	269.8	−2.68	−67.7	−5.22
$(CH_3)_2NH$	−216.6	269.8	−2.41	−61.0	−5.39
$(CH_3)_3N$	−220.8	269.8	−1.34	−54.4	−4.06

[a] See Aue et al. (42).

$$\Delta G_4 - \Delta G_1 = -\Delta G_2(R_3N) - \Delta G_2(H^+) + \Delta G_3(R_3NH^+)$$

Recall also that the solution $pK_a = -\log K_{as} = \Delta G_4^0/2.3$ RT. When the gas phase basicities were measured and showed a regular order, it was clear that the irregular order in solution was caused by a solvation effect. In the gas phase, NH_3 is a weaker base than $(CH_3)_3$ by about 23 kcal/mol; in solution this difference is only about 1 kcal/mol.

Table 4.4 lists the free energies appropriate to the thermodynamic cycle (Fig. 4.2) for the protonation of the amines. Two points deserve strong emphasis.

1. The magnitude of ΔG_4 is much smaller than that of AG, for protonation, because in aqueous solution, the amines must compete with H_2O for the proton; in the gas phase there is no competition.
2. As clearly analyzed by Aue et al. (42), the smaller the protonated amine, the more effectively solvated it is, and the better base it becomes compared with its relative rank in the gas phase.

5 CALCULATING FREE ENERGIES

Free energy is certainly one of the most important concepts in physical chemistry. The groundwork on calculating free energies was laid by Kirkwood (43) and Zwanzig (43), and the first key "modern" developments and applications came from the work of Postma et al. (44), Jorgensen and Ravimohan (45), Tembe and McCammon (46), and Warshel (47). The fundamentals of computational approaches to calculating free energies are reviewed by Beveridge and Mezei (48), and we attempted to exhaustively review applications up to 1993 (49).

To calculate the relative solvation free energies of molecules A and B in solvent S, we can use a thermodynamic cycle such as in Fig. 4.3. The relative solvation free energy of A and B, determined experimentally, is $\Delta\Delta G_{solv} = \Delta G_{solv}(B) - \Delta G_{solv}(A)$, and because the free energy is a state function, AAG is also = AG (S) − AG (g), which are the free energies determined by computational means by "mutating" the molecular mechanical model of A into B in solvent S and in the gas phase (g). Of course, if B consists of all "dummy" (non-interacting) atoms, this approach leads to the calculation of the absolute solvation free energies of A.

Being able to accurately calculate free energies of solvation suggests a reasonable balance in solute–solvent and solvent–solvent interactions. The next key challenge is to calculate $\Delta\Delta G_{bind}$ of guests G and G' to a host H, all in aqueous (or other) solution.

A typical cycle for free energy calculations (45) where H is a host, G is a guest, and HG is the host–guest complex is given in Fig. 4.4.

Now one requires a correct balance of solute (host)–solute (guest), solute (host or guest) -solvent, and solvent–solvent interactions to correctly calculate $\Delta\Delta G_{bind}$, although there clearly can be compensating errors in the calculation of ΔG_{solv} and ΔG_{bind}.

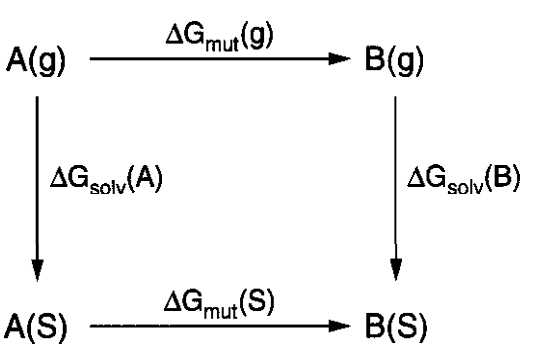


Figure 4.3. Basic thermodynamic cycle for solvation free energy.

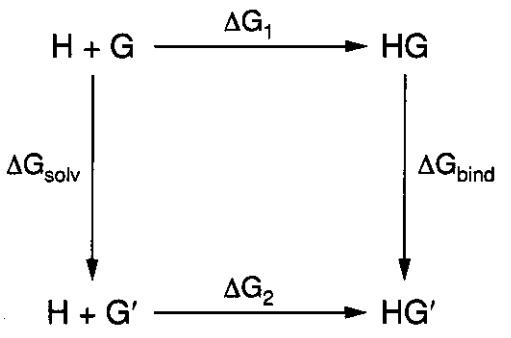


Figure 4.4. Thermodynamic cycle for host–guest interactions.

6 EXAMPLES OF DRUG-RECEPTOR INTERACTIONS

We discuss three examples of "drug target" interactions: (1)biotin-avidin (2) dihydrofolate reductase-trimethoprim, and (3)DNA-intercalator. The first is the strongest characterized protein–ligand association, the second a prototype enzyme–inhibitor interaction, and the third describes drugs interacting with nucleic acids.

6.1 Biotin-Avidin

Biotin (Fig. 4.5) is involved in the strongest known non-covalent macromolecule–ligand interaction. In fact, given the small size of biotin, it is surprising to many that this association is so strong (Ka $\sim 10^{15}$ corresponding to a –AG of $\sim$20 kcdmol) (50). The X-ray structure of streptavidin (a related protein to avidin with nearly as large a biotin affinity) biotin complex has been solved (51). The ureido group of biotin was thought to be the reason for the uniquely strong binding of this ligand to (strept)avidin.

We have carried out free energy calculations (13) on the relative binding of biotin, aminobiotin, and thiobiotin to streptavidin, as well as absolute free energy calculations of biotin binding. The results of these simulations are instructive in the insight they give us into this association. These free energy calculations can best be understood by considering the thermodynamic cycle in Fig 4.6. The free energy calculations enable one to determine the free energies of the vertical processes by mutating one ligand into another in solution (ΔG_{solv}) and when bound in the active site (ΔG_{bind}), using molecular dynamics to create an ensemble average of the system. The difference between these calculated free energies $\Delta\Delta G_{bind}$ is equal to the difference in the observed relative free energies of ligand binding.

The biotin–streptavidin system provides a "textbook case" of the relative free energies of the binding of biotin, aminobiotin, and thiobiotin, as illustrated in Table 4.5. First, the calculated relative free energies are in reasonable agreement with experiment; thiobiotin is calculated and observed to bind $\sim 10^3$ or $\sim$4 kcal/mol more weakly to streptavidin than biotin, and iminobiotin is calculated and observed to bind $\sim 10^5$ or $\sim$7 kcdmol more weakly than biotin. What is more interesting are the energy components. Thiobiotin is easier to desolvate than biotin by $\sim$9 kcal/mol (ΔG_{solv}) but interacts more weakly with the protein by $\sim$13 kcal/mol, leading to the observed $\approx$4 kcal/mol preference for biotin binding. On the other hand, iminobiotin is $\sim$5 kcal/mol harder to desolvate than biotin, but interacts only $\sim$2 kcal/mol more weakly with streptavidin, thus leading $\Delta\Delta G_{bind} = \Delta G_{bind} - \Delta G_{solv} = 2 - (-5)$ to

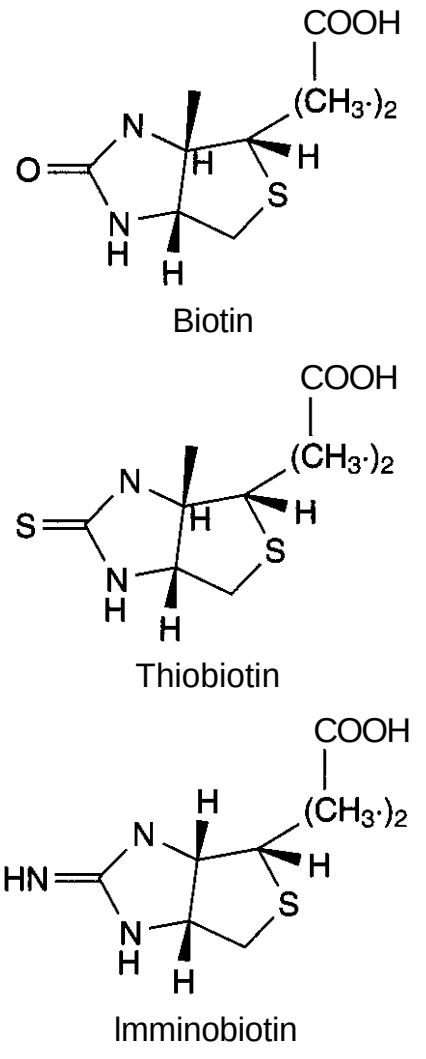
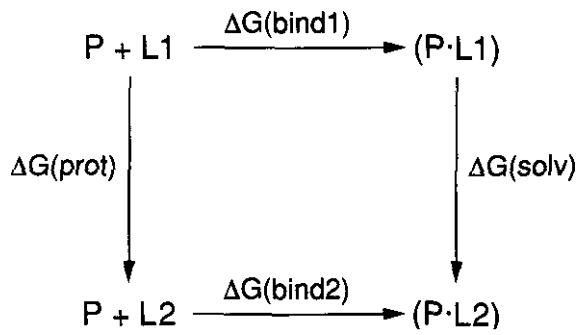


Figure 4.5. Structures of biotin and two analogs.



$$\Delta\Delta G_{bind} = \Delta G_{bind2} - \Delta G_{bind1} = \Delta G_{prot} - \Delta G_{solv}$$

Figure 4.6. Thermodynamic cycle for protein-ligand interactions. The experimentally measurable free energies are ΔG_{bind1} and ΔG_{bind1} (horizontal), and the calculated values (ΔG_{solv} and ΔG_{prot}) are the vertical processes.

its ≈7 kcallmol weaker binding to streptavidin than biotin. The above examples illustrate the interesting tradeoff in binding and solvation effects in analysis of ligand–macromolecule interactions.

The fact that one loses only 4–7 kcal/mol out of the ~20 kcal/mol in free energy of binding when mutating the ureido group to its thio and imino analog is strongly suggestive that the "ureido resonance," suggested by the crystallographers (50) who solved the structure as the reason for the unusually high K_{as}, cannot be the main reason. Calculations on the absolute free energy of biotin–streptavidin binding suggest that electrostatic effects, which might include ureido resonance (although perhaps not all of it), contribute ~6 kcal/mol to $\Delta\Delta G_{bind}$, whereas van der Waals effects contribute ~14 kcallmol.

The large contribution of van der Waals interactions (dispersion plus exchange repulsion) is surprising to many, because an individual van der Waals atom–atom dispersion attraction is very small. But there are many of them in the streptavidin active site, which, not coincidentally, contains four tryptophan residues.

But why don't the van der Waals interactions with water lost when one moves biotin from water to the streptavidin active site cancel with those gained in the active site? This can be understood by noting, as Sun et al. (52) and Rao and Singh (53) have, that a unique aspect of water as a solvent is its large exchange repulsion contribution to ΔG_{solv}. This exchange repulsion contribution represents the "hydrophobic effect," the fact that methane is less stable by 2 kcal/mol at a 1 M standard state in water than in the gas phase. This exchange repulsion cancels (and sometimes outweighs) the dispersion attraction that occurs for any solute when transferred from the gas phase to a condensed phase. On the other hand, in the streptavidin binding site, preorganized during protein synthesis, one gains dispersion attraction when biotin binds without the compensation from exchange repulsion. The magnitude of this effect is heightened by the large "atom density" both in biotin, with its bicyclic structure and in streptavidin, with its four tryptophan residues. Thus, the key aspects in biotin's tight binding with (strept)avidin is the preorganization and high atom density of the protein active site (54).

Recently, Dixit and Chipot (55) have re-examined this problem, using the improved power of modern computers to expand the sampling of configurations. The results continue to be in good accord with experiments and offer a modern paradigm for how the convergence of these simulations can be monitored.

Table 4.5 Results of Relative Free Energy Calculations[a] (kcal/mol)

			$\Delta\Delta G_{bind}$	
Perturbation	ΔG_{solv}	ΔG_{prot}	Calc. $\Delta G_{prot} - \Delta G_{solv}$	Exp[b] $\Delta G_{bind2} - \Delta G_{bind1}$
Biotin → thiobiotin	8.8 ± 0.1	12.0 ± 0.3	3.2 ± 0.3	3.6
Biotin → iminobiotin	−5.3 ± 0.1	1.2 ± 0.7	6.5 ± 0.8	6.2

[a]Errors, where listed, correspond to half the hysteresis between forward and reverse runs.
[b]Experimental data, Ref. 51.

6.2 Dihydrofolate Reductase–Trimethoprim

A classic example of a drug that works by species-specific protein inhibition is trimethoprim (TMP). Because this drug binds to bacterial dihydrofolate reductase (DHFR) $\sim 10^4$ more tightly than to the mammalian enzyme, there is a therapeutic concentration in which the drug can be used as an antibacterial with little deleterious consequences for a mammalian host.

DHFR was the first example where one has solved the X-ray crystal structure of the enzyme protein complexes for both bacteria and mammalian enzymes. Matthews et al. (56) have suggested that it is a key hydrogen bond involving the pyrimidine ring of TMP, which is present in the bacterial but not mammalian enzyme complex, that is responsible for the selectivity. This has not been definitively established with carboxyclic analogs, but analogs have clearly shown an important role of the three methoxy groups in TMP in causing species selectivity. For example, the TMP analog without the three OCH_3 groups have a binding preference for the bacterial enzyme of only ~ 10.

Kuyper (57) has analyzed the structure of the bacterial and mammalian complexes and suggested that the oxygens of the $-OCH_3$ group plays a key role in species selectivity. The methoxy oxygens are significantly more solvent exposed in the bacterial complex that the mammalian. Thus, because these oxygens do not form hydrogen bonds to enzyme groups in either complex, the desolvation penalty for the oxygen is smaller in the bacterial enzyme and does not as extensively cancel the favorable hydrophobic1 dispersion effects on binding of the methoxy methyl groups. This interpretation is supported by the fact that replacing the $-OCH_3$ with CH_2CH_3 makes the molecules less species selective; such analogs bind only a little better to bacterial DHFR but significantly better to mammalian DHFR (58, 59).

Free energy calculations/molecular dynamics have and will continue to give interesting insight into the DHFR–TMP species selectivity (39–41).

6.3 Nucleotide Intercalator

Because our first two examples have emphasized protein–small molecule interactions, we turn to a nucleic acid–small molecule interaction for our last example. There have been many experimental studies of the "intercalation" of flat, planar dyes into double-stranded DNA and other polynucleotides.

The flexibility of the sugar-phosphate backbone allows the intercalator to be sandwiched between the nucleotides with relatively little "strain." The interaction with polynucleotides by a wide variety of intercalators has been studied by physicochemical techniques. The driving force for association can be primarily hydrophobic, as in actinomycin D, where the driving force for association is AS" (57), or it can contain a large contribution from electrostatic effects as in ethidium bromide and adriamycin analogs, where the driving force for association is AH" (60) (Table 4.6). Both molecules have binding association constants K_{as} to DNA of about 10^6. The role of dispersion binding is not clear at this point, but it is likely to be very important as well (13). As noted above, the ability of these drugs to interfere with DNA replication is apparently related to their rate of dissociation k_r from DNA rather than to their association constant K_{as}. Muller and Crothers (2) showed that both actinomycin and actinomine had values of K_{as} similar to that of DNA, but the former had a much smaller k_r and a much greater effect on the rate of DNA replication. ▪

7 SUMMARY

The foregoing examples illustrate the likely nature of drug-receptor binding. It seems that hydrophobic and dispersion binding do contribute a substantial amount to the net binding affinity. However we have noted some cases (e.g., the ureido group in biotin and the intercalation of

Table 4.6 Thermodynamics of Binding of Drugs to DNA

Drug[a]	AH° (kcal/mol)	ΔS° (eu)	ΔG° (kcal/mol)
Proflavin	–6.7	+4.7	–8.1
Ethidium bromide	–6.2	+9.4	–9.0
Actinomycin D	+2.0	+39.0	–9.6
Daunomycin	–6.5	+7.7	–8.8

[a] Conditions in all cases as follow: T = 25°, 0.01 M buffer, pH = 7, I = 0.015 [see Quadrifoglio and Crescenzi (60)].

positively charged groups into DNA) in which there might be an important polar or electrostatic driving force for binding. Again, it is difficult to ascertain whether these polar contributions come from "freeing up" water or from direct interactions, but they seem to contribute in a significant fashion to the driving force for association as well as being important in determining biological specificity. The lessons for the medicinal chemist attempting to design a drug to maximize the drug receptor association include the following:

1. Conformational flexibility can decrease the association constants in a straightforwardly predictable way.
2. Hydrophobic effects usually contribute significantly to drug-receptor association, but one must also consider possible specific polar and ionic interactions.
3. Preorganization of the receptor or ligand is a key to obtaining optimal electrostatic or van der Waals interactions.

We have tried to provide examples in this chapter both of the qualitative arguments that are important for understanding ligand–protein or ligand–DNA interactions and of some typical numerical results arising from computer experiments. Understanding these interactions is key to the rational design of inhibitors, and a computer-aided approach is increasingly being used to screen libraries of potential inhibitors and to suggest improvements to lead compounds (61). As force fields and sampling methods improve and as computers become ever-more powerful, the practical use of methods like these should improve as well.

AUTHOR'S NOTE:

Peter Kollman died unexpectedly in May, 2001. He had authored an article on "Drug-Target Binding Forces" for the Fifth Edition of this series. This revision and extension for the Sixth Edition is based primarily on Peter's writings, and is dedicated to his memory.

REFERENCES

1. P. Atkins, ***Physical Chemistry,*** 4th ed., W. H. Freeman, New York, **1990.**
2. W. Muller and D. Crothers, ***J. Mol. Biol.,*** **35,251 (1968).**
3. K. Kitaura and K. Morokuma, ***Int. J. Quant. Chem.,*** **10,325 (1976).**
4. J. C. G. M. van Duijnevelt-van der Rijdt and F. B. van Duijneveldt, ***J. Am. Chem. Soc.,*** **93, 5644 (1971).**
5. J. Hirschfelder, C. Curtiss, and R. Bird, ***Molecular Theory of Gases and Liquids,*** Wiley, New York, **1954.**
6. R. H. Margenau and N. Kestner, ***Theory of Intermolecular Forces,*** 2nd ed., Pergamon Press, Oxford, **1971.**
7. H. Umeyama and K. Morokuma, ***J. Am. Chem. Soc.,*** **99, 1316 (1977).**
8. R. Lefevre, ***Adv. Phys. Org. Chem.,*** **3, 1 (1965).**
9. H. Umeyama and K. Morokuma, ***J. Am. Chem. Soc.,*** **98,4400 (1976).**
10. P. Kollman and L. C. Allen, ***Chem. Rev.,*** **72,283 (1972).**
11. M. Hanna, ***J. Am. Chem. Soc.,*** **90,285 (1968);** ***R.*** Lefevre, D. V. Radford, and P. Stiles, ***J. Chem. Soc. B,*** **31, 1297 (1968).**
12. M. Karplus and R. Porter, ***Atoms and Molecules,*** Benjamin, Menlo Park, CA, **1971.**
13. K. C. Janda, J. C. Hemminger, J. W. Winna, S. E. Novick, S. J. Harris, and W. Klemperer, ***J. Chem. Phys.,*** **63,1419 (1975);** M. Joesten and L. Schaad, ***Hydrogen Bonding,*** Dekker, New York, **1974;** K. Morokuma, S. Iwata, and W. Lathan in R. Daubel and B. Pullman, Eds., ***The World of Quantum Chemistry,*** D. Reidel, Dordrecht, Holland, **1974,** p. **277.**
14. P. Kollman. ***J. Am. Chem. Soc.,*** **99,4875 (1977).**
15. G. E. Bacon, N. A. Curry, and S. A. Wilson, ***Proc. R. Soc. Ser. A,*** **279,** 98 **(1964).**
16. S. J. Weiner, P. A. Kollman, D. A. Case, U. C. Singh, C. Ghio, G. Alagona, S. Profeta, and P. Weiner, ***J. Amer. Chem. Soc.,*** **106, 765 (1984).**
17. A. McCammon and S. Harvey, ***Molecular Dynamics*** of ***Proteins and Nucleic Acids,*** Cambridge University Press, Cambridge, UK, **1987.**
18. U. Bukert and N. L. Allinger, ***Molecular Mechanic,*** American Chemical Society, Washington, DC, **1982.**
19. W. D. Cornell, P. Cieplak, C. I. Bayly, I. R. Gould, K. M. Merz Jr., D. M. Ferguson, D. C. Spellmeyer, T. Fox, J. W. Caldwell, and P. A. Kollman, ***J. Am. Chem. Soc.,*** **117,5179 (1995).**
20. A. D. MacKerell Jr., D. Bashford, M. Bellott, R. L. Dunback Jr., J. D. Evanseck, M. J. Field, S. Fischer, J. Gao, H. Guo, S. Ha, D. Joseph-McCarthy, L. Kuchnir, K. Kuczera, F. T. K. Lau, C.

Mattos, S. Michnick, T. Ngo, D. T. Nguyen, *B.* Prodhom, *W. E. Reiher* III, *B.* Roux, *M.* Schlenkrich, *J. C. Smith, R. Stote, J. Straub, M.* Watanabe, *J. Wirkiewicz-Kuczera, D. Yin, and M. Karplus. J. Phys. Chem. B,* **102,3586 (1998).**

21. *W. L. Jorgensen, J. Chandrasekhar, J. Madura, R. W. Impey, and M. L. Klein, J. Chem. Phys.,* **79,926** (1983).
22. *H. J. C. Berendsen, J. R. Giegera, and T. Straatsma, J. Phys. Chem.,* **91, 6269** (1987).
23. *D.* L. *Veenstra, D. M. Ferguson, and P. A. Kollman, J. Comput. Chem.,* **8,971** (1992).
24. J. *Pirssette and E.* Kochanski, *J.* Am. *Chem. Soc.,* **100,6609** (1978).
25. *W.* L. *Jorgensen and* J. *Tirado-Rives, J. Am. Chem. Soc.,* **110,1657** (1988); *W.* L. *Jorgensen, D. S. Maxwell, and J. Tirado-Rives, J. Am. Chern. Soc.,* **118,11225 (1996);** G. *Kaminski and W. L. Jorgensen, J. Phys. Chem.,* **100, 18010 (1996);** *T. Fox and P. A. Kollman, J. Phys. Chem. B,* **102,8070** (1998).
26. *E. C. Meng, P. Cieplak, J. W. Caldwell, and P. A. Kollman, J. Am. Chem. Soc.,* **116,12061** (1994).
27. J. *W. Caldwell and P. A. Kollman, J. Am. Chem. Soc.,* **117,4177** (1995).
28. *J.* W. *Caldwell and P. A. Kollman, J. Phys. Chem.,* **99, 6208 (1995).**
29. Y. *Sun,* J. *W. Caldwell, and P. A. Kollman, J. Phys. Chem.,* **99, 10081** (1995).
30. R. *W.* Dixon *and P. A. Kollman, J. Comput. Chem.,* **18, 1632 (1997).**
31. *D. M. York, A. Wlodawer, L. Petersen, and T. A. Darden, Proc. Natl. Acad. Sci. USA,* **91, 8715** (1994).
32. T. E. CheathamIII, *J.* L. *Miller, T. Fox, T. A. Darden, and P. A. Kollman, J. Am. Chem. Soc.,* **117,4193 (1995).**
33. *N. Davidson, Statistical Mechanics,* McGraw-Hill, *New York,* **1962;** *M. I. Page and W. P. Jencks, Proc. Natl. Acad. Sci. USA,* **68, 1678 (1971).**
34. C. *Hansch, Biological Correlations—The Hansch Approach, ACS, Washington,* DC,1973.
35. *W. Kauzmann, Adv. Protein Chem.,* **14, 1 (1975);** *C.* Tanford, *The Hydrophobic Effect, Wiley, New York,* **1973.**
36. *W. Jencks, Catalysis in Chemistry and Enzymology,* McGraw-Hill, *New York,* **1969.**
37. *K. Dill, Biochemistry,* **29, 7133 (1990).**
38. *W. Jorgensen, J. K. Buckner, S. Boudon, and J. Tirado-Rives, J. Chem. Phys.,* **89, 3742 (1988).**
39. L. X. *Dang,* J. *Rice, and P. Kollman, J. Chem. Phys.,* **93,7528 (1990).**
40. *W. Jorgensen, J. Amer. Chem. Soc.,* **111, 3770 (1989).**
41. J. *Timko, S. Moore, D. Walba, P.* Hiberty, *and D. Cram, J. Am. Chem. Soc.,* **99,4207 (1977).**
42. *D. Aue,* H. *Webb, and M. Bowers, J. Am. Chem. Soc.,* **31,318** (1976).
43. *J. Kirkwood,* **J.** *Chem. Phys.,* **3, 300** (1935); *R. Zwanzig,* **J.** *Chem. Phys.,* **22, 1420 (1954).**
44. **J. P.** *M.* Postma, *H. J. C. Berendsen, and J. R. Houk, Faraday Symp. Chem. Soc.,* **17, 55 (1982).**
45. *W. Jorgensen and C. Ravimohan, J. Chem. Phys.,* **83,3050** (1985).
46. *B.* L. *Tembe and* J. *A.* McCammon, *J. Comput. Chem.,* **8,281 (1984).**
47. *A. Warshel, J. Phys. Chern.,* **86,2218** (1982).
48. *D.* L. *Beveridge and M. Mezei, Annu. Reu. Biophys. Chem.,* **18,431** (1989).
49. *P. A. Kollman, Chem. Rev.,* **93,2395** (1993).
50. *N. Green, Biochem. J.,* **101,774 (1966).**
51. *P. C. Weber,* J. *J. Ohlendorf, and F. R. Salemne, Science,* **243, 85 (1989).**
52. *Y. Sun, D. Spellmeyer, D. Pearlman, and P. Kollman, J. Amer. Chem. Soc.,* **114, 6798 (1992).**
53. *B. C. Rao and U. C. Singh, J. Amer. Chem. Soc.,* **111, 3125** (1989); *B. C.* Rao *and U. C. Singh, J. Amer. Chem. Soc.,* **112, 3803** (1990).
54. *S. Miyamoto and P. Kollman, Proc. Natl. Acad. Sci. USA,* **8402 (1993);** *S. Miyarnoto and P. Kollman, Proteins,* **16,226 (1993).**
55. *S. B.* Dixit *and C.* Chipot, *J. Phys. Chern. A,* **105, 9795 (2001);** *B. Kuhn and P. A. Kollman, J. Am. Chem. Soc.,* **122, 3909 (2000).**
56. *D. Matthews,* J. *Bolin,* J. *Burridge, D.* Filman, *K. Volz, B. Kaufman, C.* Beddell, *J. Champness, D. Stammers, and J. Kraut, J. Biol. Chem.,* **260, 381** (1985).
57. L. *Kuyper in C. Bugg and S. Ealick, Eds., Crystallographic and Molecular Modeling in Drug Design, Springer-Verlag,* NY, **1989,** *pp.* **56-79.**
58. *S. Fleischman and C. L. Brooks, Proteins,* **7, 52 (1990);** *C.* L. *Brooks and S. Fleischman, J. Amer. Chem. Soc.,* **112,3307 (1990).**
59. *J.* J. *McDonald and C. L. Brooks, J. Amer. Chem. Soc.,* **113, 2295 (1991);** J. J. *McDonald and C. L. Brooks, J. Amer. Chem. Soc.,* **114, 2062 (1992).**
60. *F. Quadrifoglio and V. Crescenzi, Biophys. Chem.,* **1, 319 (1974);** *F. Quadrifoglio and V. Crescenzi, Biophys. Chem.,* **2, 64** (1974).
61. *T.* J. A. *Ewing, S.* Makino, *A.* G. Skillman, *and I. D. Kuntz, J. Comput. Aided Mol. Des.,* **15,411 (2001).**